Scientia Iranica C (2023) 30(6), 2070–2081

Sharif University of Technology
Scientia Iranica
Transactions C: Chemistry and Chemical Engineering
http://scientiairanica.sharif.edu

CFD simulation of the laboratory-scale anaerobic digester to study the impacts of impeller geometric and operational parameters on its performance

M.E. Kashfi[a], R. Kouhikamali[a,b,*], G. Khayati[c], and J. Mahmoudimehr[a]

a. *Faculty of Mechanical Engineering, University of Guilan, Rasht, Iran.*
b. *Department of Mechanical Engineering, Isfahan University of Technology, Isfahan, Iran.*
c. *Faculty of Chemical Engineering, University of Guilan, Rasht, Iran.*

Received 23 January 2022; received in revised form 3 November 2022; accepted 19 December 2022

KEYWORDS
Mechanical mixing;
Impeller design;
CFD technique;
Wastewater;
Power input.

Abstract. This study numerically surveys the effects of several main parameters of an agitated anaerobic digester on mixing rate and power input. Numerical simulation is conducted employing the Finite Volume Method (FVM), and it is validated with available experimental data. The results indicate that doubling the blade length enhances the mixing rate and the power input by 39.9% and 13.5 times, respectively; increasing the number of blades (from 4 to 6) improves the mixing rate by 12.5% and makes the power input grow 1.4 times; and decreasing the blade tilt angle from 45° to 30° causes the mixing rate to drop by 14% and decreases the power input 1.8 times. Furthermore, the observations show that the mixing rate and power input are adversely influenced by the wastewater concentration. At last, the most effective impeller design, among 144 cases investigated, is found and suggested.

1. Introduction

Promoting awareness of global warming and rising energy prices have brought more attention to renewable energies in recent years. This kind of energy can be obtained from different types of renewable sources (such as waste and wastewater) and through the use of Anaerobic Digestion (AD) processes. AD technique is widely used in Waste Water Treatment Plant (WWTP) to improve the quality of wastewater and to stabilize the sludge produced from wastewater treatment [1]. The overall performance of the AD systems depends significantly on the mixing [2]. A proper mixing leads to uniformity of materials and temperature in wastewater and causes efficient material transfer from substrate to microorganisms in the large volume of the reactor [3]. According to investigations, methane gas production rate and effluent quality using anaerobic digesters are significantly affected by the mixing [4,5]. Furthermore, in the field of the mixing process, the quality of the mixture [6] as well as power consumption in agitated tanks [7,8] have always been concerning for researchers. There are three major mixing techniques, namely the impeller mixing [9,10], slurry recirculation [11], and gas recirculation. Each of the mentioned methods has advantages and disadvantages, and impeller mixing is the most impressive technique among the modes of mixing [12,13]. To obtain a good mixture, the Continuously Stirred Tank Reactor (CSTR) is typically used [14,15],

*. *Corresponding authors. Tel.: +98 (31)3 3915242; Fax: +98 (31)3 3912628*
E-mail addresses: mohammad_kashfi57@yahoo.com (M.E. Kashfi); r.kouhikamali@iut.ac.ir. and kouhikamali@guilan.ac.ir (R. Kouhikamali); khayati@guilan.ac.ir (G. Khayati); mahmoudimehr@guilan.ac.ir (J. Mahmoudimehr)

doi: 10.24200/sci.2022.59791.6444

and Computational Fluid Dynamics (CFD) techniques have emerged as a helpful tool to predict and model the fluid flow [16,17]. The numerical simulation can help the researcher identify the effects of several parameters, such as the geometry of the reactor, the number of blades, the tilt angle of the blade, and the rheological properties of the fluids on both flow pattern [18] and the mixing rate without the need to construct a commercial reactor.

Vesvikar and Al-Dahhan [19] numerically simulated the mixing process, which was provided by sparging gas within a digester to determine flow patterns. The numerical results were consistent with the experimental data obtained from the Computer Automated Radioactive Particle Tracking (CARPT). Buwa et al. [20] reported the numerical and experimental investigations for mixing in the tank agitated with different impellers. In this study, the mixing performance was evaluated, and the numerical results were in good agreement with experimental data. Wu [21] examined several turbulence models for non-Newtonian fluids in agitated anaerobic digesters to evaluate the power number and the flow number obtained from the CFD with those of laboratory data. Among the turbulence models studied, the realizable K-ε and the standard K-ω models were found more suitable than the others. Magelli et al. [22] reported that the dimensions and agitator types had a strong effect on the mixing time (or homogenization) of the stirred tanks. Trad et al. [23] used CFD-based simulations to investigate the impact of the agitator geometry on the flow patterns inside a digester, and the numerical results were consistent with the experimental data. Lebranchu et al. [24] studied the impacts of impeller types and shear stress on biogas production using the CFD simulation method and the results obtained from the experimental data.

Meister et al. [25] reported that for concentrated wastewaters, the K-ε model was more appropriate than the K-ω model with regard to the simulation performance. Mendoza et al. [26] performed a CFD simulation to assess the impact of impeller rotational speed and fluid viscosity on the flow fields in a stirred tank. Mao et al. [27] determined the indexes to increase the AD performance and to minimize the mixing time using CFD simulation. Müller et al. [28] attempted to optimize an externally mixed bio-gas plant through coupling of CFD simulations with optimization software. Cui et al. [29] focused on numerical simulations to reveal the impacts of various impellers on the flow field and the mixing performance within digesters. Rave et al. [30] applied a Scale-Adaptive Simulation (SAS) of single-phase flow to evaluate the flow pattern in a baffled stirred tank at a high Reynolds number and, also, illustrated the effect of the blade geometry.

According to the provided literature survey, a number of studies attempted to discover and improve the mixing pattern inside a digester; however, they realized that the impacts of several main geometric parameters (such as the blade size, the number of blades, and tilt angle of the blade) and operational parameters (such as the agitation speed and the wastewater concentration or total solid) had not been studied perfectly, especially by using an integrated approach. The current study employs UDF-assisted fluent to numerically investigate the effects of the mentioned parameters on mixing rate and determines power input (or operational cost) from the numerical solution reports in an agitated anaerobic digester. For this purpose, the Total Solids (TS) of 2.5%, 7.5%, 12.1%; the impeller diameter sizes (D) of $d/3$, $d/2$, $2d/3$, (where d denotes the digester diameter); blade tilt angles of 30°, 45°; two different numbers of blades (i.e., 4 and 6 blades); and agitation speeds of 250, 500, 750, and 1500 rpm for the cylindrical digester are investigated. Finally, the results of different settings for the design parameters are compared in terms of power input and mixing rate, which is related to power production, and the best choice is proposed.

2. Theoretical model and methods

In this study, the continuity, momentum, and turbulence equations are used to determine the hydrodynamics of flow in the agitated anaerobic digester. Due to the complexity of the AD process, the simplifying assumptions are considered as follows:

i. The behavior of the wastewater (or fluid) at a concentration of TS $\geq$ 2.5% is non-Newtonian and the wastewater is incompressible and isothermal;

ii. The realizable K-ε model is employed to characterize the turbulent flow;

iii. The standard wall functions are used for near-wall treatment;

iv. The temperature of the mixing system including the wall and the wastewater is fixed at 35°C;

v. The computations are done for a three-dimensional non-time-dependent turbulent flow.

2.1. Governing equations

2.1.1. Continuity equation

The equation of continuity is described by the following equation:

$$\frac{\partial \rho}{\partial t} + div(\rho \mathbf{V}) = 0, \tag{1}$$

herein, $\boldsymbol{V}$ (m/s) and ρ (kg/m^3) denote the velocity vector and the density of the fluid.

2.1.2. Conservation of momentum

The momentum equation is represented by the following expression:

$$\rho \frac{DV}{Dt} = -\nabla p + \nabla . \tau + \mathbf{F}. \quad (2)$$

The variables p (Pa), τ (N/m^2), and $\mathbf{F}$ (N/m^3) define the fluid's static pressure, the viscous stress tensor, and the body force vector per unit volume.

2.1.3. Turbulence equations

In this study, due to the complexity of the governing flow, the realizable K-ε model is used to describe the turbulent flow characteristics in which K (m^2/s^2) and ε (m^2/s^3) denote the turbulence kinetic energy and the turbulence dissipation rate, respectively; these parameters are defined by the following transport equations:

$$\rho \frac{DK}{Dt} = \nabla \left[\left(\mu + \frac{\mu_t}{\sigma_k} \right) \nabla K \right] + G_k - \rho \varepsilon, \quad (3)$$

$$\rho \frac{D\varepsilon}{Dt} = \nabla \left[\left(\mu + \frac{\mu_t}{\sigma_\varepsilon} \right) \nabla \varepsilon \right] + \rho C_1 S \varepsilon - \rho C_2 \frac{\varepsilon^2}{K + \sqrt{\vartheta \varepsilon}}, \quad (4)$$

where G_k (J/m^{3}s) and μ_t (Pas) denote the generation of turbulence kinetic energy due to the mean velocity gradients and the eddy viscosity; the model constant values (dimensionless) C_2, σ_k, and σ_ε are equal to 1.9, 1, and 1.2, respectively. Also, C_1 is defined as follows:

$$C_1 = \max \left[0.43, \frac{\delta}{\delta + 5} \right]. \quad (5)$$

Herein, $\delta = S\frac{K}{\varepsilon}$ and S (s^{-1}) denotes the modulus of the mean strain rate [31].

2.1.4. Non-Newtonian fluid model

As mentioned, the behavior of the wastewater with $TS \geq 2.5\%$ can be considered as non-Newtonian. In the non-Newtonian fluid model used in the system, the rheological characteristics of wastewater depend on the TS values; therefore, these values can be obtained by the following expression [32]:

$$\eta = k . \dot{\gamma}^{n-1}, \quad (6)$$

$$\rho = 0.0367 TS^3 - 2.38 TS^2 + 14.6 TS + 1000. \quad (7)$$

The variables η (Pas) and $\dot{\gamma}$ (s^{-1}) denote the non-Newtonian viscosity and the shear rate. Also, the constants k (Pa.s$^{\mathrm{n}}$), n (dimensionless), and TS (%) define the consistency coefficient, the power-law index, and the concentration of the wastewater, respectively.

The details of rheological characteristics and densities of the wastewater with different TSs are reported in Table S1 (see supplementary material).

2.2. Description of major dimensionless parameters

The flow features within the agitated digester are affected by the impeller; therefore, the Reynolds number, Re, is determined by the following equation [33]:

$$Re = \frac{D^2 N^{2-n} \rho}{k} \left[8 \left(\frac{n}{6n+2} \right)^n \right]. \quad (8)$$

Herein, N (rps) and D (m) denote the agitation speed and diameter of the impeller, noting that the values of the constants n and k are summarized in Table S1.

In this study, the dimensionless parameter of N_p, which denotes the power number, is defined by the following equation [34]:

$$N_p = \frac{P_{in}}{\rho N^3 D^5}. \quad (9)$$

Also, the power input of the system, P_{in} (W), can be obtained from the impeller torque, T (Nm), which is determined by the CFD simulation results:

$$P_{in} = 2\pi N T. \quad (10)$$

The mixing rate (%), represented by α, is an important dimensionless parameter that is described as the ratio of the stream zone volume to the total volume of the digester. Furthermore, the stream zone is specified as the area with the velocity value greater than 5% of the maximum of the velocity of the entire computational domain [19]. After calculating the mixing rate using UFD-assisted fluent, the methane production (power production) is determined from solving the governing equations numerically [35].

The Coefficient of Performance, COP (dimensionless), is determined by the following equation:

$$\mathrm{COP} = \frac{P_{out}}{P_{in}}, \quad (11)$$

Hint: α and P_{in} are dependent on (D, θ, n, N, TS), and also P_{out} is a function of (α), where P_{out} (W) is the power production. The parameters of the objective function (COP) depend on the impeller diameter (D), the blade tilt angle (θ), the number of the blade (n), the agitation speed (N), the TS, and the mixing rate (α). The COP is applied to determine the optimal system.

2.3. Model's geometry and boundary conditions

In this section, the illustrative view of the geometry of the computational domain, meshing, and boundary conditions is given in Figure S1 (see supplementary material). To create a suitable meshing in terms of quality, due to the complex geometry of the impeller, the unstructured grids using a mixture of elements (tetrahedral and triangular) are generated in ANSYS workbench. A steady-state modeling approach called the Multiple Reference Frame (MRF) is employed to describe the rotational flow created by the impeller, noting that in this model, the flow field calculations in the bulk area (including all the domains in the computational zone except impeller) are determined by using the agitation speed, which is equal to the speed of the impeller. The geometric data of the laboratory

Table 1. Dimensions of laboratory-scale cylindrical digester, impeller, and MRF.

Parameters	Values (cm)
Digester diameter	17.4
Digester height	26
Impeller diameter size	6.2
Blade height	1.5
Blade thickness	0.3
Dist. from bottom	8.6
D_{MRF}	9
$H_{impeller}$	2.2

-scale cylindrical digester, impeller, and the MRF size are summarized in Table 1.

2.4. Numerical solution technique

To discretize and solve the governing equations in the mixing model, the Finite Volume Method (FVM) is performed through ANSYS fluent commercial software (Ver. 17.1) [36]. The velocity-pressure coupled differential equations are solved by using the SIMPLE algorithm. In this regard, initially, for solving the governing equations such as momentum and turbulence equations, the first-order upwind scheme of about 100 iterations is done. At last, the mentioned equations are solved through the second-order upwind scheme. To achieve the convergence criterion, the residual values below 10^{-4} are employed for continuity, V_x, V_y, V_z, K, and ε in fluent.

2.5. Mesh study

In order to investigate the grid independence for the numerical solution of the mixing model in the current study, the CFD simulation of the model (for $TS = 7.5\%$ and an agitation speed of 1500 rpm) is done for different grid numbers (585455, 953551, 1759752, and 2247207 cells), and the effects of the grid numbers on the velocity magnitude at different points around the impeller zone as well as the mixing rate are checked. By comparing the obtained results from CFD simulation of the mixing model in terms of the velocity values, which were previously reported by Kashfi et al. [35], and the mixing rate (see Table 2), among the four grids studied, it can be concluded that the model with the grid number of 1759752 cells is determined to be adequately fine; in this grid conditions, grid independence can be ensured by checking with higher resolution grids (2247207 cells).

Table 2. Grid independence analysis regarding mixing rate (α).

No.	Number of cells	α (%)	Difference (%)
1	585455	99.76	–
2	953551	98.8	1
3	1759752	97.5	1.3
4	2247207	97.4	0.1

3. Validation of CFD simulation

To confirm the numerical simulation in terms of the numerical method accuracy, the CFD simulation results are compared with the available experimental data published by Hoffmann et al. [37]. The reasons for using Hoffmann's model are its geometry similarities (such as impeller diameter, the geometry of the reactor, and the impeller type) to the present work geometry. To this end, the radial velocity values are measured in the impeller zone (or z = 50 mm) at two agitation speeds of impeller (i.e., 250 and 500 rpm) and also, at the points obtained with the average difference percentages of 5% and 4%, respectively (for more details, see Figure S2 in the supplementary material). It is found that the CFD simulation results are consistent with the experimental data. Hence, the CFD technique applied in this research can well predict the flow patterns.

4. Results and discussion

This section surveys the effects of various main geometric and non-geometric parameters of mechanically agitated anaerobic digester on the mixing rate and power input as two major objective functions. The main geometric parameters, including impeller diameter size ($d/3$, $d/2$, $2d/3$), number of blades (4 and 6), and blade tilt angle (30°, 45°), agitation speed (250, 500, 750, 1500 rpm), and wastewater concentration ($TS = 2.5\%$, 7.5%, 12.1%) are the non-geometric parameters. Since the power input is related to the power number (see Eq. (9)), the reports of power number are presented in this section.

4.1. The effect of impeller geometry on the mixing rate and power number

The geometric characteristics of the impeller are the most considerable factors affecting the mixing rate and the power number. Herein, the impacts of the blade size, the number of blades, and the blade tilt angle are studied. The effect of the impeller geometric features on the mixing rate and power number is shown in Figure 1.

4.1.1. The effect of the size of the blade

Figure 1(a) shows the effect of the length of the blade on the mixing rate of the system, while blade tilt angle, number of blades, and TS are set at 45°, 4, and 7.5%, respectively. This figure indicates that increasing the length of the blade, which increases the hydraulic diameter (or the impeller diameter), has led to a larger volume of wastewater to be swept and greater momentum to be penetrated into the lateral and upper layers of the digester. This observation was reported

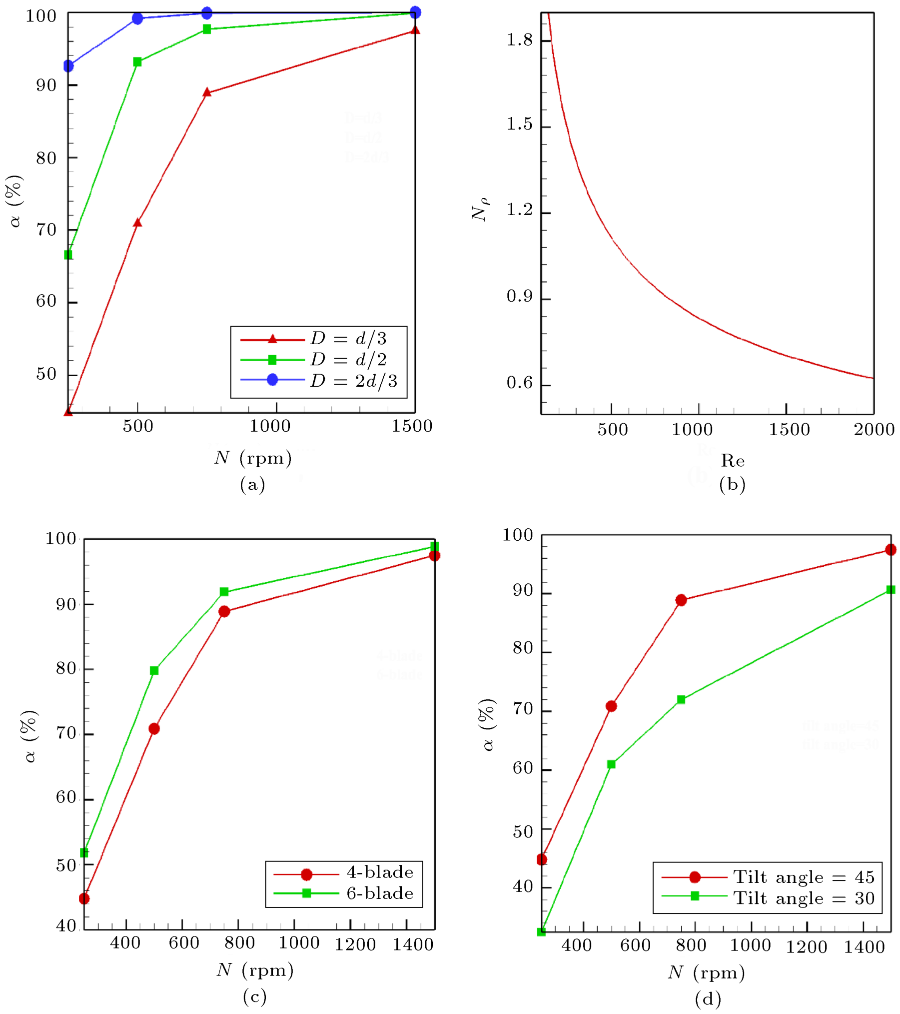

Figure 1. Effect of (a) impeller diameter size on mixing rate, (b) impeller diameter size on power number, (c) blade number on mixing rate, and (d) blade tilt angle on mixing rate.

by Vesvikar and Al-Dahhan in another way [19]. They observed that a greater size of the blade resulted in a smaller dead zone.

The mixing rate index is not the only important engineering objective, and the power number plays an important role in the performance of the mechanical mixing system [38]. Table 3 is presented to study the effect of blade length on the system power input from the turbulence intensity (TI) point of view. This table shows that TI (maximum intensity as a representative) increases upon increasing blade length.

Table 3. Maximum Turbulent Intensity (TI) for different impeller diameter sizes[a].

Impeller diameter size	Max. TI (dimensionless)
$d/3$	0.4
$d/2$	0.61
$2d/3$	0.76

[a](4-blade, 500 rpm, 45° and $TS = 7.5\%$).

The dimensionless parameter of TI is determined by the following equation:

$$\mathrm{TI} = \frac{\sqrt{\frac{2}{3}K}}{u}, \tag{12}$$

where K (m^2/s^2) is the turbulence kinetic energy, and u (m/s) is the mean velocity.

A greater TI is associated with higher viscous dissipation and, hence, higher energy dissipation or greater power input. Figure 1(b) shows the power number calculated at different Re numbers. As demonstrated by the predicted results, a smaller power number was observed at a higher Re number. This indicates that the more power input took place in the case of a larger blade because the kinetic energy in the impeller was proportional to the fifth-order impeller diameter (see Eq. (9)).

4.1.2. The effect of the number of blades

Figure 1(c) depicts the effect of the number of blades on the mixing rate within the agitated digester. As shown,

Table 4. Power number for different numbers of blades[a].

Number of blade	N (rpm)	N_p
4	250	1.36
6	250	1.8
4	500	1.22
6	500	1.68

[a]($D = d/3$, 45°and $TS = 7.5\%$).

Table 5. Power number for different blade tilt angles[a].

Tilt angle (°)	N (rpm)	N_p
45	250	1.36
30	250	0.84
45	500	1.22
30	500	0.68

[a]($D = d/3$, 4-blade and $TS = 7.5\%$).

at a fixed speed, the higher number of blades has led to a greater mixing rate. This is because for the higher number of blades, a larger surface area is in contact with the wastewater and therefore, a larger volume of wastewater is affected by the impellers. In addition, Table 4 reports the variations of the power number versus the number of blades. This table indicates the direct dependence of power number on the number of blades, which was previously shown by Nagata et al. [39]. Furthermore, it can be concluded that there is a direct relationship between power number and power input. This is because the kinetic energy in the impeller remained constant for the same speed and blade size.

4.1.3. The effect of the tilt angle of the blade

The influence of blade tilt angle on mixing rate is shown in Figure 1(d). Herein, impeller diameter size, number of blades, and TS are set at $d/3$, 4, and 7.5%, respectively. Figure 1(d) shows that for the same rotational speed, the tilt angle of 30° resulted in a lower mixing rate than the tilt angle of 45°. This occurrence can be attributed to the fact that a lower tilt angle, which is equivalent to a higher deviation of the blades from the flow direction, causes a smaller volume of the wastewater-swept region to rotate with the impeller. Therefore, it is expected that the penetration of momentum into the digester and consequently, the mixing rate of the system would decrease. The power number at different blade tilt angles is listed in Table 5. As observed, at the same rotational speed, by reducing the tilt angle of the blade, the power number decreases. Because of the higher deviation of the blade from the flow direction (by changing the tilt angle from 45° to 30°), it is expected that lower resistance would occur in the opposite direction of rotation. Therefore, this indicates that decreasing the blade tilt angle from 45° to 30° can reduce the power input. This observation was previously confirmed by Major-Godlewska and Karcz [40].

4.2. The effect of agitation speed on the mixing rate and power number

The axial flow impeller is used in this research. This impeller can create flows parallel to the axis of the impeller stator and is suitable for creating vertical flows [41]. Figure 2(a)–(d) show the contours of velocity value within the computational domain at different agitation speeds, while impeller diameter size, tilt angle, number of blades, and TS are considered fixed at $d/3$, 45°, 4, and 7.5%, respectively. The figure indicates that with increase in the agitation speed, the momentum diffusion to the lateral and upper layers of the wastewater increased. Therefore, the wastewater mixing rate is observed to be positively affected by increasing the agitation speed. This trend remains intact for other geometric conditions and rheological properties of the wastewater; this issue is not reiterated for the sake of brevity. For illustration, increasing the agitation speed from 250 to 1500 rpm has led the mixing rate to increase from 44.8% to 97.5%. By using nonlinear regression in this case, the $\alpha - N$ function can be obtained:

$$\alpha = 30.142 ln(N) - 117.91. \tag{13}$$

Herein, α (%) and N (rpm) denote the mixing rate and the rotational speed of the impeller, and the value of the coefficient of determination, R^2, is sufficient ($R^2 = 0.9422$).

In the studied conditions, if the mixing rate of the system is the same as the value obtained at 1500 rpm of the impeller (equal to 97.5%) according to Eq. (13), the agitation speed of the impeller will be 1270 rpm. Therefore, it can be deduced from the 1270 to 1500 rpm range that there is no change in the mixing rate of the system, and increasing the agitation speed increases only the power input of the system. Moreover, to calculate the minimum agitation speed, a mixing rate of 5% is allocated in the above equation. The impeller speed for the mixing rate of 5% will be 59 rpm. It should be noted that the systems with agitation speeds less than this value have negative mixing rates, being conceptually insignificant. In other words, mixing does not occur in the system (or the unmixed mode). Thus, based on the numerical results, it is suggested that the agitation speeds in the range of 59 to 1270 rpm be applied to analyze the performance of this mixing system.

Figure 2(e) illustrates the power number versus Re number. As observed, for entirely turbulent flows at large Re, the system power number does not show notable changes and tends to a constant value. This prediction is in good agreement with the experimental results [34], and also this trend indicates that the higher

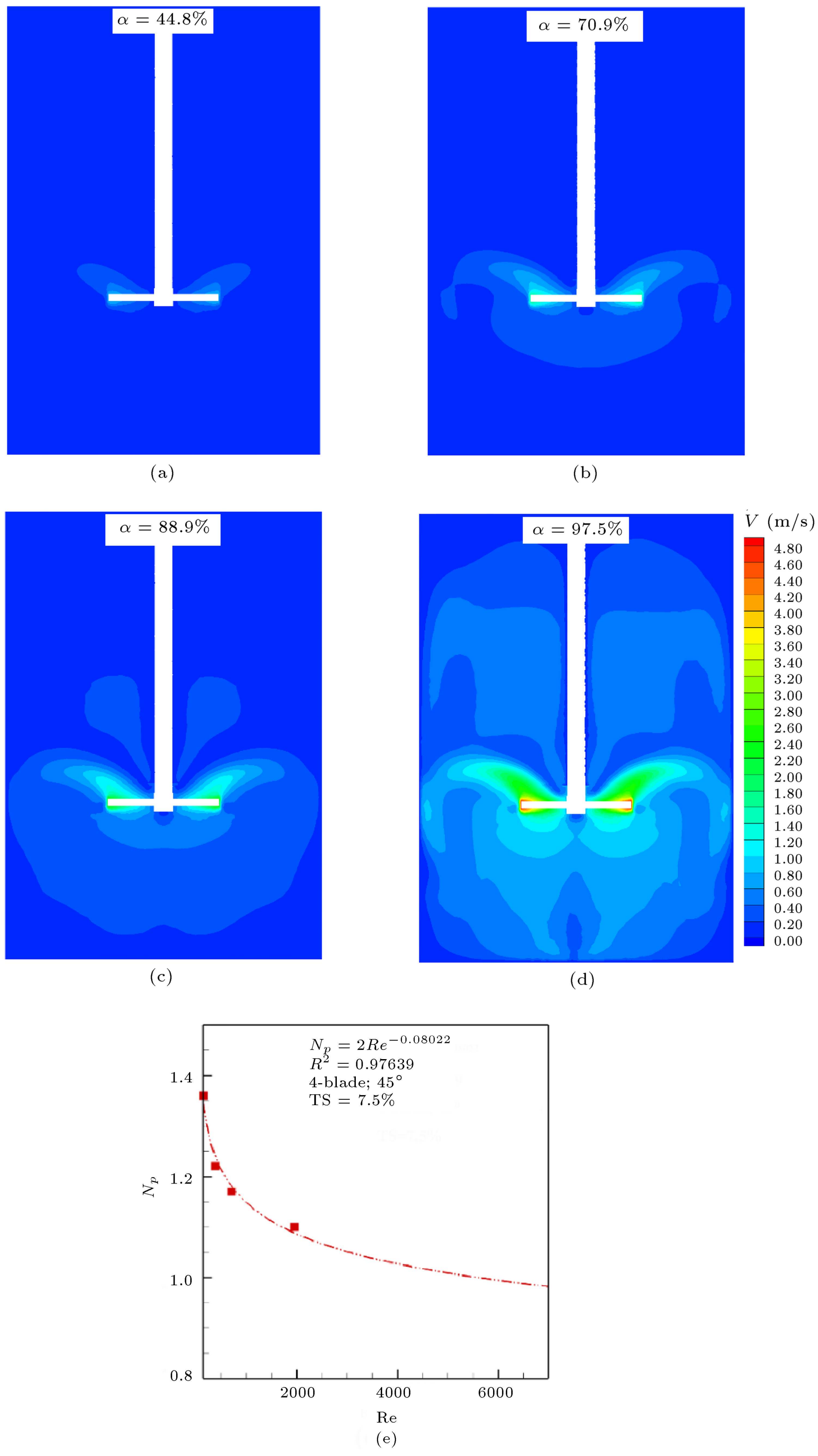

Figure 2. Contours of velocity value within the computational domain at agitation speeds of (a) 250, (b) 500, (c) 750, and (d) 1500 (rpm); Effect of agitation speed on power number for the impeller diameter size of $d/3$.

the Re number, the greater the power input due to higher impeller torque. In this case, an exponential regression between power number and Reynolds number can be observed:

$$N_p = 2Re^{-0.08022}. \tag{14}$$

Notably, the determination coefficient, R^2, is found satisfactory and larger than 0.97.

Based on the obtained results in this study, the power number predicted for impeller A-310 was equal to 0.315 under turbulent conditions, while in the same conditions, the value of 0.3 was reported in the published data by Hemrajani and Tatterson [34].

4.3. The effect of TS on the mixing rate and power number

The TS of wastewater in the system is an important parameter affecting the mixing efficiency. It influences the fluid dynamics by affecting the wastewater rheological behavior [33]. Figure 3 reveals the effect of TS on the mixing rate and the power number. Figure 3(a)–(c) show the contours of velocity value within the computational domain at different levels of TS, while the impeller diameter size, the tilt angle, the number of blades, and the agitation speed are set at $d/3$, 45°, 4, and 500 rpm, respectively.

As observed, at a higher TS, the momentum diffusion into the lateral and upper layers of the wastewater is reduced; therefore, the system mixing rate is inversely related to the TS. Furthermore, as shown in Figure 3(a)–(c), for a higher TS, the highest velocity gradient is observed in areas around the blades. The effect of TS on the power number is depicted in Figure 3(d). As can be seen, the power number in a digester with higher TS is greater than those in a digester with lower TS. It can be concluded that a higher TS value in this condition leads to greater power input due to the same kinetic energy in both

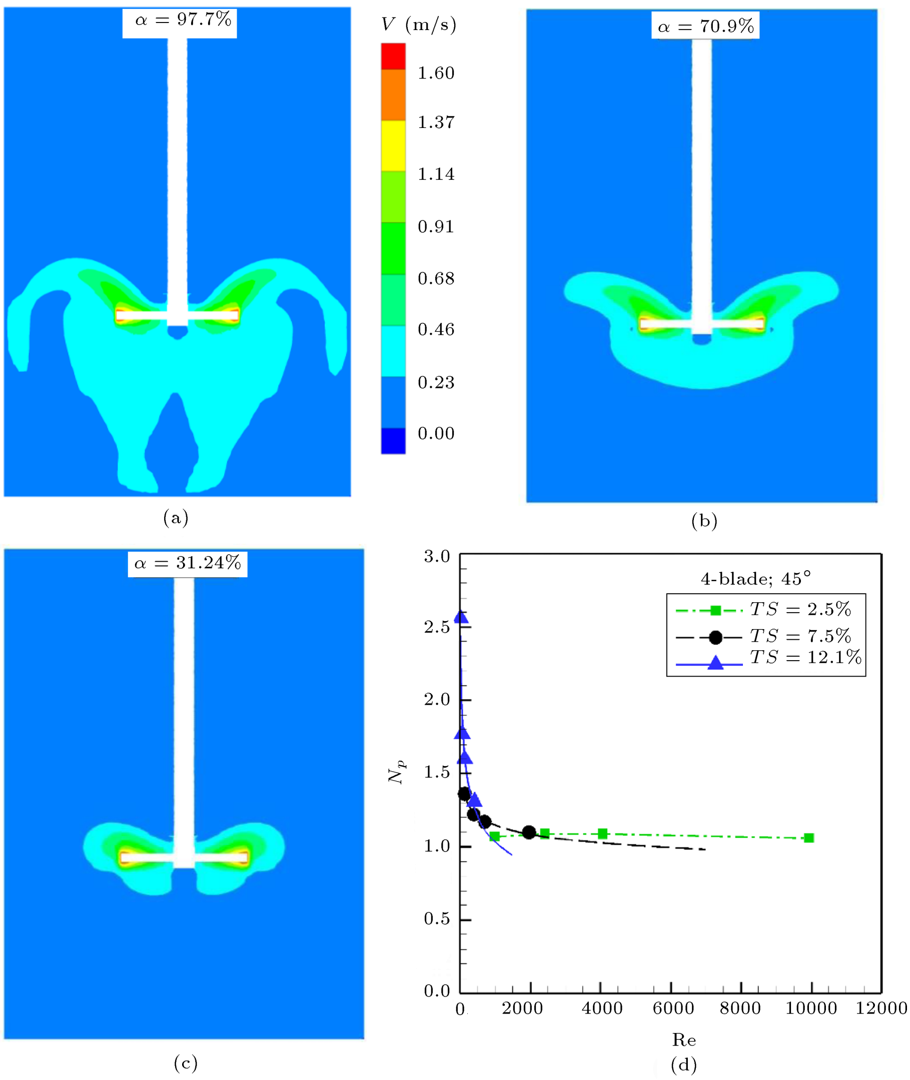

Figure 3. Contours of velocity value within the computational domain for the TS of (a) 2.5%, (b) 7.5%, and (c) 12.1%; (d) Effect of TS on power number for the impeller diameter size of $d/3$.

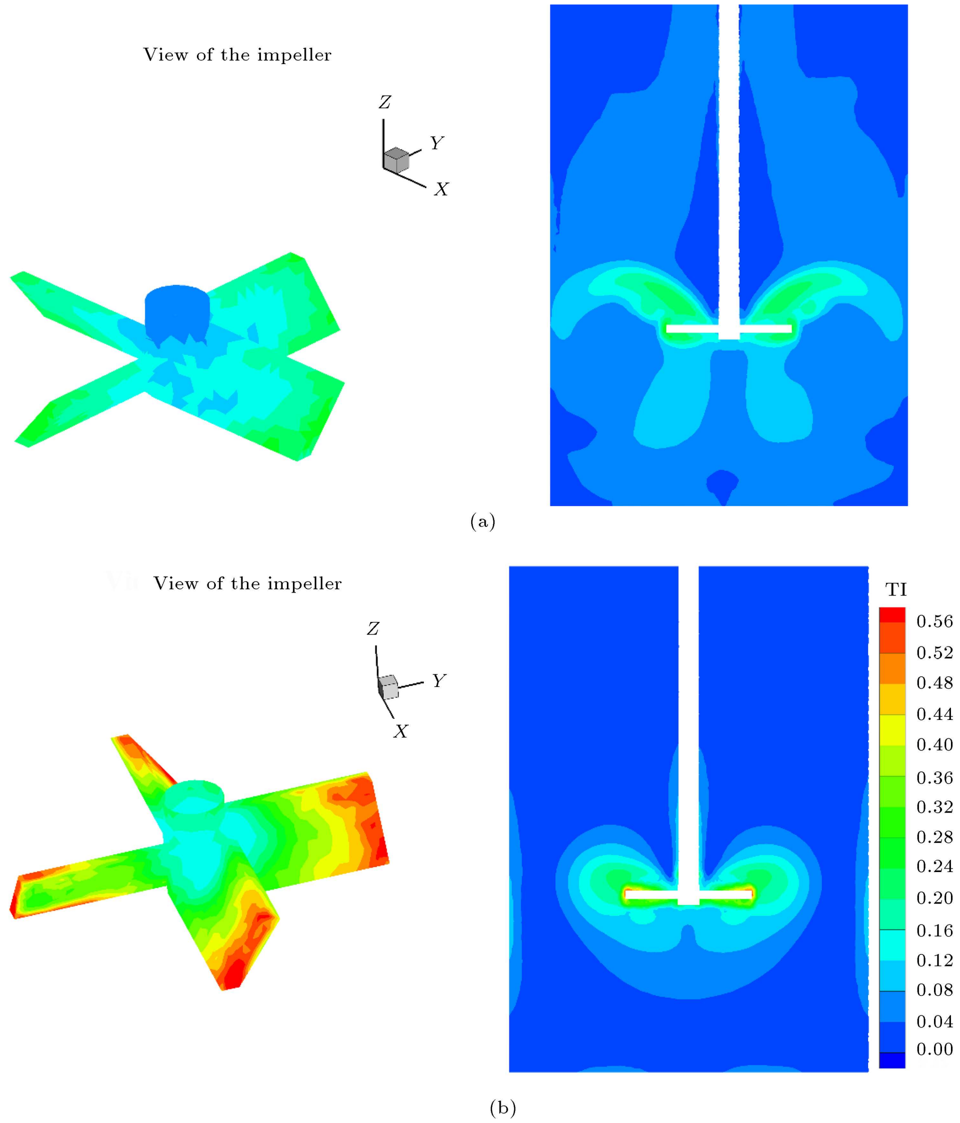

Figure 4. Contours of Turbulence Intensity (TI) within the computational domain for the TS of (a) 2.5% and (b) 12.1%.

systems. For instance, at $Re = 2000$, the predicted power input in this research is 0.32 W in a system with TS of 2.5% and 15.7 W in a system with TS of 7.5%. This observation may be attributed to the fact that the higher viscosity leads to higher viscous dissipation.

Also, the impacts of TS on the TI dimensionless parameter for concentrations 2.5% and 12.1% in the agitated anaerobic digester are studied. The investigation results are shown in Figure 4, while the diameter size, tilt angle, number of blades, and agitation speed of the impeller are considered to be set at $d/3$, 45°, 4, and 500 rpm, respectively.

As observed, the system with a higher TS leads to a higher TI. As a result, the dissipation of viscosity and energy consumption experience an increase, leading to the rise of the power input of the system. Furthermore, as can be seen in Figure 4, the highest TI gradient is seen in areas around the blades, and the movement of the fluid is done slowly toward the walls and upper layers of the digester with higher TS due to the effects of the fluid viscosity. These reasons cause the mixing rate parameter to decrease in the system with a higher TS. At last, it can be deduced that the results obtained from the TI point of view are in complete agreement with the above-presented results.

4.4. Practical application of this study

By considering the mixing rate, which is directly related to methane production and power production, and the power input as the main objectives of the present work, the number of blades, tilt angle, size, and agitation speed of the impeller equal to 4, 30°, 62 mm, and 250 rpm, respectively, form the best impeller design among the 144 models examined (see supplementary material in Table S2). Moreover, for the most efficient large-scale impeller design, it is important to simultaneously evaluate the influence of mixing on both power input and methane production; of note, it is necessary to apply the criteria of similarity such as geometric and mixing energy level, which were presented in some studies (see [42,43]). After obtaining the detailed geometric information of the anaerobic digester from the mentioned criteria, the CFD simulation can be used to simulate the flow field in real anaerobic digesters. These results are helpful in determining real mixing efficiency in the digesters.

5. Conclusions

This research numerically studied the effects of some main parameters (especially impeller geometry related ones) on the mechanical performance of an anaerobic digester. The results showed that doubling the blade size, increasing the blade tilt angle from 30° to 45°, and increasing the number of agitating blades from 4 to 6 improved the mixing rate by 39.9%, 14%, and 12.5%; however, they caused the power input to increase 13.5 times, 1.8 times, and 1.4 times, respectively. The four-blade impeller with a tilt angle of 30° and a diameter one-third of the tank diameter was found the most efficient design.

Supplementry data

file:///C:/Users/SHAMILA/Downloads/Supplementary %20material(1).pdf

References

1. Tchobanoglous, G., Burton, F.L., and Stensel, H.D., *Wastewater Engineering; Treatment and Reuse*, 4th Edn., McGraw-Hill Companies, Inc. (Metcalf and Eddy, Inc.), New York, USA (2003).
2. Wang, H., Larson, R.A., Borchardt, M., et al. "Effect of mixing duration on biogas production and methanogen distribution in an anaerobic digester", *Environ. Technol.*, **42**(1), pp. 93–99 (2019).
3. Álvarez, C., Colón, J., Lópes, A.C., et al. "Hydrodynamics of high solids anaerobic reactor: Characterization of solid segregation and liquid mixing pattern in a pilot plant VALORGA facility under different reactor geometry", *Waste Manag.*, **76**, pp. 306–314 (2018).
4. Borole, A.P., Klasson, K.T., Ridenour, W., et al. "Methane production in a 100-L upflow bioreactor by anaerobic digestion of farm waste", *Appl. Biochem. Biotechnol.*, **131**, pp. 887–896 (2006).
5. Kashfi, M., Kouhikamali, R., and Khayati, G. "The effect of mixing rate on performance of anaerobic reactor in methane production", *Iran. J. Energy Environ.*, **12**(3), pp. 209–219 (2021b).
6. Dapelo, D. and Bridgeman, J. "Assessment of mixing quality in full-scale, biogas-mixed anaerobic digestion using CFD", *Bioresour. Technol.*, **265**, pp. 480–489 (2018).
7. Mahmoodi-Eshkaftaki, M., Ebrahimi, R., and Ghasemi-Pirbaloti, A. "Design of stirred digester with optimization of energy and power consumption", *Environ. Prog. Sustain. Energy*, **36**(1), pp. 104–110 (2017).
8. Qiu, N., Wang, P., Si, Q., et al. "Scale process effect on the power consumption characteristics of a novel curved Rushton turbine within a reactor vessel", *Chem. Eng. Res. Des.*, **166**, pp. 109–120 (2021).
9. Kariyama, I.D., Zhai, X., and Wu, B. "Influence of mixing on anaerobic digestion efficiency in stirred tank digesters: A review", *Water Res.*, **143**, pp. 503–517 (2018).
10. Jaszczur, M., Młynarczykowska, A., and Demurtas, L. "Effect of impeller design on power characteristics and newtonian fluids mixing efficiency in a mechanically agitated vessel at low reynolds numbers", *Energies*, **13**(3), p. 640 (2020). https://doi.org/10.3390/en13030640.
11. Yang, D., Hu, C., Dai, L., et al. "Post-thermal hydrolysis and centrate recirculation for enhancing anaerobic digestion of sewage sludge", *Waste Manag.*, **92**, pp. 39–48 (2019).
12. Colangiuli, S., Rodríguez, A., Sanromán, M.Á., et al. "Demonstrating the viability of halolipase production at a mechanically stirred tank biological reactor", *Bioresour. Technol.*, **263**, pp. 334–339 (2018).
13. Lone, S.R., Kumar, V., Seay, J.R., et al. "Evaluation of volumetric mass transfer coefficient in a stirred tank bioreactor using response surface methodology", *Environ. Prog. Sustain. Energy*, **38**, pp. 387–401 (2019).
14. Lindmark, J., Eriksson, P., and Thorin, E. "The effects of different mixing intensities during anaerobic digestion of the organic fraction of municipal solid waste", *Waste Manag.*, **34**, pp. 1391–1397 (2014).
15. Singhal, S., Agarwal, S., Singhal, N., et al. "Designing and operation of pilot scale continuous stirred tank reactor for continuous production of bio-methane from toxic waste", *Environ. Prog. Sustain. Energy*, **38**(1), pp. 198–200 (2019).
16. Ranganathan, P. and Savithri, S. "Computational fluid dynamics simulation of hydrothermal liquefaction of microalgae in a continuous plug-flow reactor", *Bioresour. Technol.*, **258**, pp. 151–157 (2018).
17. Zamankhan, P. "Large eddy simulations of a mixing tank with axial flow turbine", *Sci. Iran.*, **14**(4), pp. 336–351 (2007).
18. Kan, K., Zheng, Y., Chen, Y., et al. "Numerical study on the internal flow characteristics of an axial-flow pump under stall conditions", *J. Mech. Sci. Technol.*, **32**, pp. 4683–4695 (2018).
19. Vesvikar, M.S. and Al-Dahhan, M. "Flow pattern visualization in a mimic anaerobic digester using CFD", *Biotechnol. Bioeng.*, **89**(6), pp. 719–732 (2005).

20. Buwa, V., Dewan, A., Nassar, A.F., et al. "Fluid dynamics and mixing of single-phase flow in a stirred vessel with a grid disc impeller: experimental and numerical investigations", *Chem. Eng. Sci.*, **61**(9), pp. 2815–2822 (2006).

21. Wu, B. "CFD investigation of turbulence models for mechanical agitation of non-Newtonian fluids in anaerobic digesters", *Water Res.*, **45**(5), pp. 2082–2094 (2011).

22. Magelli, F., Montante, G., Pinelli, D., et al. "Mixing time in high aspect ratio vessels stirred with multiple impellers", *Chem. Eng. Sci.*, **101**, pp. 712–720 (2013).

23. Trad, Z., Vial, C., Fontaine, J.P., et al. "Mixing and liquid-to-gas mass transfer under digester operating conditions", *Chem. Eng. Sci.*, **170**, pp. 606–627 (2017).

24. Lebranchu, A., Delaunay, S., Marchal, P., et al. "Impact of shear stress and impeller design on the production of biogas in anaerobic digesters", *Bioresour. Technol.*, **245**, pp. 1139–1147 (2017).

25. Meister, M., Rezavand, M., Ebner, C., et al. "Mixing non-Newtonian flows in anaerobic digesters by impellers and pumped recirculation", *Adv. Eng. Softw.*, **115**, pp. 194–203 (2018).

26. Mendoza, F., Bañales, A.L., Cid, E., et al. "Hydrodynamics in a stirred tank in the transitional flow regime", *Chem. Eng. Res. Des.*, **132**, pp. 865–880 (2018).

27. Mao, L., Zhang, J., Dai, Y., et al. "Effects of mixing time on methane production from anaerobic co-digestion of food waste and chicken manure: Experimental studies and CFD analysis", *Bioresour. Technol.*, **294**, 122177 (2019). https://doi.org/10.1016/j.biortech.2019.122177.

28. Muller, J., Schenk, C., Keicher, R., et al. "Optimization of an externally mixed biogas plant using a robust CFD method", *Comput. Electron. Agric.*, **171**, 105294 (2020).

29. Cui, M.H., Zheng, Z.Y., Yang, M., et al. "Revealing hydrodynamics and energy efficiency of mixing for high-solid anaerobic digestion of waste activated sludge", *Waste Manag.*, **121**, pp. 1–10 (2021).

30. Rave, K., Lehmenkuhler, M., Wirz, D., et al. "3D flow simulation of a baffled stirred tank for an assessment of geometry simplifications and a scale-adaptive turbulence model", *Chem. Eng. Sci.,* **231**, 116262 (2021). https://doi.org/10.1016/j.ces.2020.116262.

31. Shih, T.H., Liou, W.W., Shabbir, A., et al. "A new $k-\varepsilon$ eddy viscosity model for high Reynolds number turbulent flows", *Comput. Fluids*, **24**(3), pp. 227–238 (1995).

32. Leonzio, G. "Study of mixing systems and geometric configurations for anaerobic digesters using CFD analysis", *Renew. Energy*, **123**, pp. 578–589 (2018).

33. Yu, L., Ma, J., and Chen, S. "Numerical simulation of mechanical mixing in high solid anaerobic digester", *Bioresour. Technol.*, **102**(2), pp. 1012–1018 (2011).

34. Hemrajani, R.R. and Tatterson, G.B. "Mechanically stirred vessels", In *Handbook of Industrial Mixing: Science and Practice*, E.L. Paul, V.A. Atiemo-Obeng and S.M. Kresta, Eds., pp. 345–390, John Wiley and Sons Inc., New Jersey, USA (2003).

35. Kashfi, M.E., Kouhikamali, R., and Khayati, G. "Simultaneous evaluation of the effect of mixing efficiency on power consumption and methane production in an anaerobic digester with different wastewaters", *Bioresour. Technol.*, **338**, 125554 (2021a). https://doi.org/10.1016/j.biortech.2021.125554.

36. ANSYS Fluent "ANSYS Fluent 17.0 User's Guide", Canonsburg, Penn. ANSYS, Inc., USA (2016).

37. Hoffmann, R.A., Garcia, M.L., Veskivar, M., et al. "Effect of shear on performance and microbial ecology of continuously stirred anaerobic digesters treating animal manure", *Biotechnol. Bioeng.*, **100**(1), pp. 38–48 (2008).

38. Chudacek, M.W. "Impeller power numbers and impeller flow numbers in profiled bottom tanks", *Ind. Eng. Chem. Process Des. Dev.*, **24**(3), pp. 858–867 (1985).

39. Nagata, S., Nishikawa, M., Tada, H., et al. "Power consumption of mixing impellers in pseudoplastic liquids", *J. Chem. Eng. Jpn.*, **4**(1), pp. 72–76 (1971).

40. Major-Godlewska, M. and Karcz, J. "Power consumption for an agitated vessel equipped with pitched blade turbine and short baffles", *Chem. Pap.*, **72**, pp. 1081–1088 (2018).

41. Wu, J. and Pullum, L. "Performance analysis of xaial-flow mixing impellers", *AIChE J.*, **46**(3), pp. 489–498 (2000).

42. Stukenberg, J.R., Clark, J.H., Sandine, J., et al. "Egg-shaped digesters: from Germany to the U.S", *Water Environ. Technol.*, **4**(4), pp. 42–51 (1992).

43. Wu, B. "CFD simulation of mixing in egg-shaped anaerobic digesters", *Water Res.*, **44**(5), pp. 1507–1519 (2010).

Biographies

Mohammad Esmaeel Kashfi received his MSc and PhD degrees in Mechanical Engineering-Energy Conversion from the University of Guilan, Iran in 2015 and 2022, respectively. His main research interests include the design and CFD simulation of mixing systems, renewable energy, and non-Newtonian fluid flows.

Ramin Kouhikamali received his PhD degree in Mechanical Engineering-Energy Conversion from Amirkabir University of Technology, Iran in 2008. He is currently a Professor at the Department of Thermo-Fluids, Isfahan University of Technology. His main research interests include the experimental and numerical study of two-phase flows, desalination units, water treatment, and renewable energy. He is the author and co-author of many papers in these fields.

Gholam Khayati is currently an Associate Professor of Chemical Engineering at the University of Guilan. His main research interests are bioseparation and wastewater treatment. He has presented many research articles in various journals in these fields.

Javad Mahmoudimehr received his BSc degree in Mechanical Engineering from the University of Guilan, Iran in 2004. He earned his MSc and PhD degrees at Iran University of Science & Technology, Iran in 2007 and 2012, respectively. He is currently an Associate Professor at the Mechanical Engineering Faculty, University of Guilan. His research interest fields include energy, optimization, and renewable energy. He has published many papers in different journals in these fields.